Adhesion in NiAl-Cr from first principles

James E. Raynolds
Department of Materials Science and Engineering, University of Michigan, Ann Arbor, Michigan 48109-2136

John R. Smith
Department of Physics and Physical Chemistry, General Motors Research Laboratories, Warren, Michigan 48090

G.-L. Zhao* and David J. Srolovitz
Department of Materials Science and Engineering, University of Michigan, Ann Arbor, Michigan 48109-2136

(Received 13 November 1995)

Fully self-consistent all-electron density functional calculations have been performed to obtain the full adhesion curves for the systems NiAl, Cr, and NiAl-Cr. We find that the work of adhesion for Cr is larger than that for NiAl and for the interface between these two materials the work of adhesion is intermediate. We find that NiAl at the NiAl-Cr interface is Ni-terminated. Electronic charge density distributions indicate that the bonding is largely metallic with a discernible covalent character. The interfacial bonding is due largely to the Ni and Cr *d* electrons while in NiAl the bonding results from *sp-d* hybridization. Estimates of segregation effects suggest a reduction of the work of adhesion for the interface by roughly 20%. Comparisons between our calculated ideal work of adhesion and fracture toughness measurements indicate that significant crack-tip plasticity is associated with the brittle fracture mechanism of NiAl. Our results are consistent with previous electronic structure calculations and measurements on NiAl and fracture mechanisms observed for NiAl-Cr composites.

I. INTRODUCTION

There is considerable interest in nickel aluminide (NiAl) composites composed of refractory metal (such as Cr) reinforcements in a NiAl matrix because these materials show promise for use in high-temperature structural applications.[1–3] NiAl forms in the cesium chloride structure (one atom type at cube corners, the other at body centers) and has a high melting temperature (1911 K), high thermal conductivity (4–8 times that of Ni-based super alloys), is resistant to oxidation, and is of relatively low density (5.9 g/cm^2 at room temperature).[4,5] Unfortunately, however, it is too brittle at and below room temperature and has relatively poor elevated temperature (>1000 K) strength. This precludes the use of pure NiAl as a structural material in many applications since the thermal stresses produced during temperature cycling would likely lead to crack growth. Composites which retain the desirable high temperature properties of NiAl but show increased ductility at low temperatures can be formed by adding refractory metals to NiAl. The present study is concerned primarily with NiAl matrices reinforced with Cr.

Eutectic composites, in which microscopic fibers (rods) or lamellae (plates) of Cr form in the NiAl matrix, have been produced by directional solidification of $(NiAl)_{66}Cr_{34}$.[1,2,6–11] The morphology is easily changed from fibrous to lamellar by adding small amounts of Mo, V, or W.[7] The directional solidification process aligns the fibers (or lamellae) along the growth direction and leads to increased high temperature strength. In these composites, the NiAl (CsCl structure) and Cr (bcc) crystal axes are all parallel (cube on cube) and the interfaces between these two phases are semicoherent (i.e., large separation exists between dislocations). Due to the near perfect lattice matching ($\delta a_0 \ll 1\%$), the density of misfit dislocations is low (spacing on the order of 0.07 μm).[2]

The room temperature fracture resistance (fracture toughness) of NiAl-Cr eutectic composites is over three times that of pure NiAl because good bond strength between the NiAl- and Cr-rich phases prevents them from acting independently. It is the adhesion between phases that is the subject of this paper. This adhesion leads to several toughening mechanisms: crack bridging, crack deflection, and an increased supply of mobile dislocations produced at the interface by thermal cycling and the difference in thermal expansion coefficients of the NiAl- and Cr-rich phases.[1,2] Another source of toughening arises because of the difference in fracture planes for the two materials. The fracture plane for NiAl is of the {110} type whereas for Cr the fracture planes are of the {001} type. A crack must, therefore, change direction when entering a new phase. The degree to which the Cr can deform depends on how it is constrained by the NiAl matrix. Increasing the degree of debonding at the NiAl-Cr interface leads to an increase in the volume of the Cr phase that can deform and hence the amount of work needed to fracture the Cr increases.

The ideal work of adhesion for the NiAl-Cr interface (i.e., the energy required to rigidly cleave the interface) is a quantity of fundamental importance for understanding the strength and fracture characteristics of NiAl-Cr composites. The Griffith model[12] for the ideal fracture strength of brittle solids states that cracks will propagate if it is energetically favorable for them to do so. Elastic energy stored in the strained material ahead of the crack is released as the crack moves. If the magnitude of this energy is greater than the surface energy required to create new surface as the crack is

opened (i.e., the crack faces), the crack will propagate. The Griffith model relates the critical stress for crack propagation σ_F to the crack length c and work of adhesion W_{ad} as

$$\sigma_F = \left(\frac{W_{\mathrm{ad}} E}{\pi c} \right)^{1/2}, \tag{1}$$

where E is Young's modulus. This result is significant in that an expression similar in form to Eq. (1) applies even for situations in which limited plastic deformation is associated with crack propagation. In such a case, Eq. (1) is modified by replacing W_{ad} by $W_{\mathrm{ad}} + W_p$ where W_p is the plastic work associated with dislocation motion and other nonelastic deformation. The plastic work W_p is indirectly related to W_{ad} since the amount of plastic work achievable is determined by the magnitude of the stresses near the crack tip and these stresses are limited by the bond strength (work of adhesion) at the crack tip. Since it is very difficult to measure W_{ad} for the internal interfaces of the eutectic composites, we employ theoretical methods to determine W_{ad}.

In this paper we present the results of first principles electronic structure calculations to determine the ideal work of adhesion W_{ad} and peak interfacial stress $\sigma_{\max}$ of NiAl, Cr, and NiAl-Cr, as well as the electronic properties related to bonding (such as electronic charge density rearrangements and densities of states). The purpose of this study is to determine the magnitude of the work of adhesion of a NiAl-Cr interface and to determine the underlying bonding characteristics. A self-consistent first principles solution is essential to an accurate description of interfacial bonding, bond breaking, and surface formation which occurs upon separating the interface, since considerable electronic charge rearrangement occurs.

II. DENSITY FUNCTIONAL CALCULATIONS

We represent the interface between NiAl and Cr as that between two lattice matched thin slabs for which no in-plane atomic relaxation is allowed. The lattice constant is fixed at the experimental value which is reported to be 2.88 Å for both NiAl- and Cr.[9,10] Since the goal of the present study is to establish trends in ideal chemical bond strengths, we do not explicitly consider the effects of atomic relaxation around the interface. Therefore the work of adhesion discussed herein is referred to as the *ideal work of adhesion*. Since only {001} surfaces and interfaces are considered here, we expect that the work of adhesion and the *ideal* work of adhesion will differ by only a few percent. This follows from the observation that the relaxation of high-symmetry surfaces in relatively close-packed metallic systems is small. Use of the ideal work of adhesion allows us to unambiguously separate the energy of fracture into a reversible part and a dissipative part associated with plastic deformation. Either definition of the work of adhesion should suffice since, as is shown below, the work associated with plasticity is nearly 200 times the value of the ideal work of adhesion.

Our unit cell consists of five layers of NiAl sandwiched between two outer three-layer slabs of Cr. This arrangement was chosen for computational efficiency since it allows a mirror symmetry plane through the center of the NiAl slab to reduce the computational effort. The layers, which extend infinitely in the x and y directions, are stacked along the {001} (i.e., z) direction. Above and below the Cr/NiAl/Cr computational cell are several layers of vacuum. Figure 1 depicts our computational half unit cell in which periodic boundary conditions are assumed in the x and y directions and the mirror symmetry plane coincides with the lowest plane of atoms in the figure. Half the experimental lattice constant [(2.88 Å)/2] is used for the interplane spacing in each slab. Experience has shown that, due to the short screening lengths associated with metallic systems, these slabs are sufficiently thick that the adhesion curves (i.e., energy vs interslab spacing) do not show finite size effects.[13–15] Evidence supporting this claim for the present system will be presented in the following section.

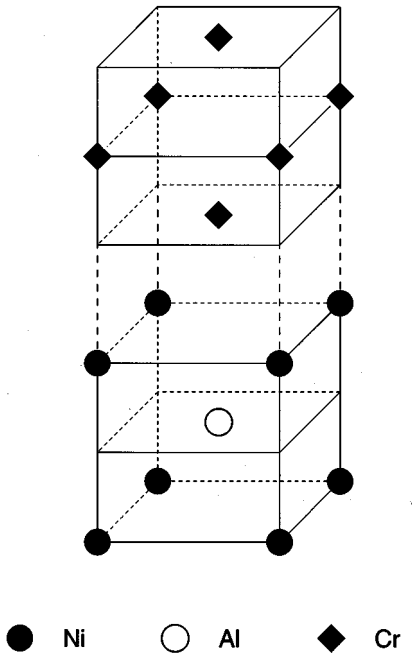

FIG. 1. Half unit cell used to study interfacial adhesion between NiAl and Cr. Periodic boundary conditions in the x and y directions are employed and a mirror symmetry plane coincides with the layer atoms at the bottom of the figure. The unit cell extends beyond the top of the figure to include enough vacuum to isolate the system from its periodic images along the z direction. The adhesion energy curve is obtained by calculating the total energy as the Cr subsystem is displaced relative to the NiAl subsystem.

The energy of the system at different interslab separations is determined by calculating the paramagnetic ground state at each separation using the self-consistent local-orbital (SCLO) method. This method solves the electronic ground state problem in the local-density approximation[16] (LDA) in a basis of atomic orbitals. We obtain the atomic orbitals by performing self-consistent all-electron calculations on isolated atoms and fitting the results with sets of even-tempered Gaussians. The minimum basis set obtained in this way is augmented by including additional, more diffuse, basis functions (polarization functions) for each atom. The resulting set corresponds to the chemist's ''double-ζ plus polarization'' basis. The frozen core approximation[17] is adopted and the Ceperley-Alder exchange-correlation potential[18] is used to generate the Hamiltonian matrix for the entire system in a basis of Bloch functions (superpositions of atomic orbitals) indexed by the in-plane momentum ($k_{\parallel}$). The problem is

solved by diagonalizing the Hamiltonian matrix, updating the potential, and iterating to self-consistency. We optimize the exponents for the polarization functions to minimize the total energy of a several-layers-thick slab. For this optimization we used a three-layer slab for Cr and for NiAl we used two different three-layer slabs, one with Ni atoms on the surface and one with Al atoms on the surface. The exponents for the rest of the basis were fixed at the values given by the fits to the atomic calculations. Calculated work functions provided a further check of the quality of the basis. For further details of the SCLO method see Ref. 19. Finally, we obtain the adhesion curve by plotting the total calculated energy vs interfacial separation.

The calculated adhesion energy curve (energy vs separation) is fitted to a universal-binding-energy relation[13] (UBER). The UBER is commonly parametrized as

$$E=-E_0(1+a^*)e^{-a^*}=-\frac{W_{\mathrm{ad}}}{2}(1+a^*)e^{-a^*}, \qquad (2)$$

where

$$a^*=(d-d_0)/l, \qquad (3)$$

E is the total energy per unit surface area [not to be confused with Young's modulus of Eq. (1)], and d is the interfacial separation. Equation (2) has been found to apply to a large class of metallic and covalently bonded systems.[20] In the above equations, E_0 is the ideal adhesion energy which for pure systems (NiAl or Cr separately) is equal to the surface energy (γ). The ideal work of adhesion is therefore related to the ideal adhesion energy as $W_{\mathrm{ad}}=2E_0$. In Eq. (3), d_0 is the equilibrium interfacial separation and l, the scaling length, is a fitting parameter which is related to the elastic properties of the material. The interfacial stress σ vs separation is obtained by differentiating Eq. (2) with respect to interfacial separation:

$$\sigma=\sigma_{\max}a^*e^{(1-a^*)}. \qquad (4)$$

In Eq. (4), the peak interfacial stress $\sigma_{\max}$ is related to the ideal adhesion energy E_0 and the scaling length l by

$$\sigma_{\max}=\frac{2E_0}{le}, \qquad (5)$$

where e is the base of the natural logarithm.

III. RESULTS AND DISCUSSION

A. Adhesion energy and stress

The calculated adhesion curves for NiAl and Cr (Fig. 2) along a {001} plane are of the UBER form [Eq. (2)]. These results imply that the ideal work of adhesion along a {001} plane is larger for Cr than for NiAl. Figure 2 also contains data for the NiAl/Cr and AlNi/Cr interfaces, where we have adopted the notation that the NiAl at the NiAl/Cr interface is Al terminated while NiAl is Ni-terminated at the AlNi/Cr interface. These data demonstrate that the work of adhesion of the Ni-terminated AlNi/Cr interface is larger than that for the Al-terminated interface. This suggests that NiAl at a {001} NiAl-Cr interface is preferentially Ni terminated and, hence, we shall exclusively consider this interface. The work

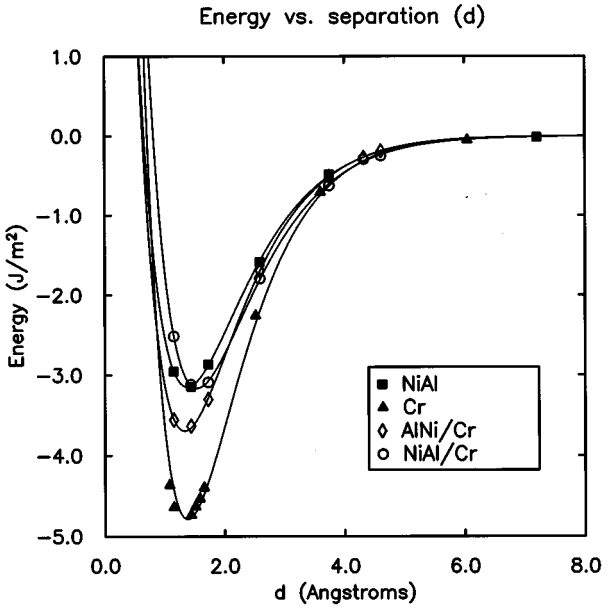

FIG. 2. Calculated total energy (per interfacial area) vs interfacial separation (d) for the systems NiAl, Cr, and NiAl-Cr. These results suggest that the work of adhesion for NiAl-Cr is intermediate between Cr (the highest) and NiAl (the lowest) and that it is energetically more favorable for Ni rather than Al to be in contact with Cr (i.e., the interface is Ni-terminated). In each case the interface is a plane whose normal is parallel to the {001} crystallographic direction. The curve designated AlNi/Cr was calculated with Ni in contact with the Cr while NiAl/Cr corresponds to having Al in contact with the Cr. For each system, the solid curve is a fit obtained using the universal-binding-energy relation of Eq. (2).

of adhesion of the AlNi/Cr interface is intermediate between that of NiAl and Cr. The ideal work of adhesion results are summarized in Table I. Table I also includes the calculated surface energies of the individual phases.

The ideal interfacial stress vs separation (Fig. 3) follows the same trend as for the work of adhesion in that Cr has the highest peak interfacial stress, NiAl the lowest, and that for NiAl-Cr is intermediate between NiAl and Cr. The peak interfacial stress for NiAl is very close in value to that for the Al-terminated interface (NiAl/Cr) with the latter slightly larger than the former. Close agreement between the work of adhesion for these two systems also exists. The similarity between the Al-terminated interface and NiAl reflects the strong similarity between the bonding characteristics of Ni and Cr. Table II summarizes the fitting parameters for the

TABLE I. Calculated works of adhesion W_{ad} (J/m^2), for NiAl, Cr, and NiAl-Cr. Surface energies $E_{\mathrm{surf}}=W_{\mathrm{ad}}/2$ are given for the pure systems NiAl and Cr. The calculated works of adhesion are ordered: $W_{\mathrm{ad}}^{\mathrm{Cr}}>W_{\mathrm{ad}}^{\mathrm{AlNi/Cr}}>W_{\mathrm{ad}}^{\mathrm{NiAl/Cr}}>W_{\mathrm{ad}}^{\mathrm{NiAl}}$.

System	E_{surf}	W_{ad}
NiAl	3.2	6.3
Cr	4.8	9.6
NiAl/Cr		6.3
AlNi/Cr		7.4

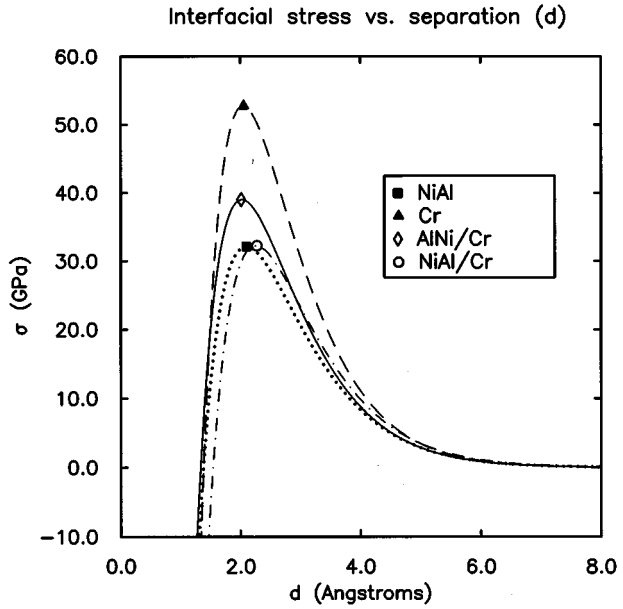

FIG. 3. Calculated ideal interfacial stress vs separation for the systems NiAl, Cr, and NiAl-Cr. These curves were obtained by differentiating the UBER curves for the adhesion energy of Fig. 2. These results imply that Cr has the highest peak interfacial stress (corresponding to the the highest tensile strength), NiAl has the lowest, and NiAl-Cr (AlNi/Cr) has a value intermediate between Cr and NiAl. Also, AlNi/Cr (Ni-terminated interface) is stronger than NiAl/Cr (Al-terminated interface).

UBER. The trends for the peak stresses can easily be seen by inspection of the first row of Table II.

The equilibrium interfacial separation d_0 and scaling length l also give some indication as to the nature of the interfacial bonding. For instance, the stronger Ni-terminated interface (AlNi/Cr) has a smaller interfacial separation than the Al-terminated interface. Likewise the stronger pure material, Cr, has a smaller d_0 than does NiAl. The trend for the scaling length l closely follows the stress and energy trends. The stronger interfaces have shorter values of l and the scaling lengths for NiAl and NiAl/Cr are the same, reflecting the similarities between Al-Cr and Al-Ni bonds. The correlation between E_0, $\sigma_{\max}$, d_0, and l is given by Eq. (5), which should be viewed as the theoretical strength at the atomic level, whereas the Griffith model in Eq. (1) provides the nominal stress at fracture of a macroscopic sample containing a sharp crack of length c. Note that the values of d_0 for NiAl and Cr are as much as 0.1 Å smaller than the measured value of 1.44 Å. This underestimate of interfacial bond lengths is common to LDA calculations and is primarily due to the LDA.

TABLE II. Calculated peak interfacial stress $\sigma_{\max}$ (GPa), equilibrium interfacial separation d_0 (Å), and scaling length l (Å) for the systems NiAl, Cr, and NiAl-Cr. The following trend is observed: $\sigma_{\max}^{\mathrm{Cr}} > \sigma_{\max}^{\mathrm{AlNi/Cr}} > \sigma_{\max}^{\mathrm{NiAl}}$ for the peak interfacial stress.

	NiAl	Cr	NiAl/Cr	AlNi/Cr
$\sigma_{\max}$	32.1	52.8	32.3	39.0
d_0	1.38	1.33	1.54	1.33
l	0.72	0.67	0.72	0.70

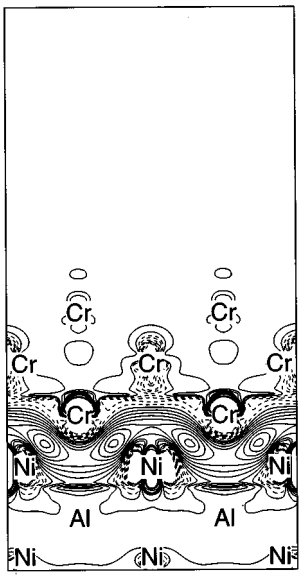

FIG. 4. Charge density rearrangements which arise upon forming the NiAl-Cr interface from isolated NiAl and Cr crystals. Electronic charge density distributions for the separated slabs were subtracted from that for the combined system. Solid curves represent charge accumulation and dashed curves represent charge depletion. Displayed are the results for the plane normal to the {110} direction for the half unit cell. The continuous band of charge which accumulates is indicative of metallic bonding while the significant pileup of charge along the lines connecting Ni and Cr atoms suggests a covalent character to the bonding.

At this point a few comments regarding improvements to the theory which go beyond the LDA are in order. The LDA is only formally valid for systems in which the charge density is a slowly varying function of the spatial coordinates. The fact that the LDA works so well outside the domain of formal validity is due to cancelation of errors.[21] Methods such as the so-called generalized gradient correction (GGA) approach, which go beyond the LDA, work well in situations where the exchange-correlation hole (the charge density rearrangement around an electron due to exchange and correlation) is localized near the associated electron such as is the case in a bulk solid. For this reason, bulk properties such as lattice constants and bulk moduli are better represented in the GGA theory than in the LDA.[22] However, surface energies are not improved by the use of the GGA.[22,23] Therefore we do not expect GGA's to significantly change the calculated work of adhesion relative to that obtained with the LDA.

B. Electronic properties

Electronic charge density rearrangements which occur upon forming the interface from isolated crystals indicate that the interfacial bonding is largely metallic while some covalent character is also evident. Figure 4 is a contour plot obtained by subtracting the electronic charge distribution for the equilibrium interfacial separation from that at large interfacial separation. Solid contours indicate charge accumulation and dashed contours represent charge depletion. The contours range from $-1.2\ e/\mathrm{a.u.}^3$ to $+1.1\ e/\mathrm{a.u.}^3$ and adjacent contours represent values which differ by $0.14\ e/\mathrm{a.u.}^3$.

The continuous band of charge which accumulates along the interface indicates metallic bonding. There is, in addition, a significant accumulation along the lines connecting the interface Ni and Cr atoms which suggests a partial covalent character to the interfacial bonding.

A Mulliken orbital population analysis[24] of the orbitals contributing to AlNi/Cr interfacial bonding shows that the valence $3d$ states play a significant role in the interfacial bonding.[25] The largest changes in orbital population for the Ni interface atoms which occur upon forming the interface are as follows. The population of the $3d_{z^2-r^2}$ and $3d_{x^2-y^2}$ states increases by 0.24 e/a.u.^{3} while the population of the $3xz$, $3yz$, and $3xy$ decreases by roughly the same amount (0.18 e/a.u.^{3}). The filling of the polarization $5s$ state decreases by 0.19 e/a.u.^{3}, roughly the same amount as the changes for the $3d$ states. The sum of the populations for the valence $4s$ and $4p$ states increases by 0.21 e/a.u.^{3} which is about this amount. Changes of this magnitude for the interfacial Cr atoms occur for the valence $4s$ and polarization $5s$ states, which decrease in occupancy. The absolute value of the changes for the Cr $3d$ states, 0.07 e/a.u.^{3}, is roughly an order of magnitude smaller than those for the interfacial Ni. While the valence $4p$ occupations increase by 0.15 e/a.u.^{3} for Ni and 0.23 e/a.u.^{3} for Cr — roughly the same amount for both Ni and Cr — the Cr $4s$ occupation changes by -0.23 e/a.u.^{3} which is roughly -3 times the change for Ni $4s$.

As always, care must be taken when interpreting results of a Mulliken population analysis so as not to read too much significance into any particular numerical value but only to use the results to ascertain trends in bonding. This is because there is no unique way to assign spectral weight to any given orbital. Thus to the extent to which a Mulliken population analysis can be trusted we can summarize the previous discussion as follows. The interfacial bonding between Ni and Cr atoms is due to the $3d$, $4p$, $4s$, and $5s$ states. The largest changes in orbital population upon forming the interface occur for the Ni $3d$ and $5s$ states, while for Cr the largest changes occur for the $4s$ and $5s$ states with the changes for $3d$ and $4p$ states down by roughly a factor of 2 from those for the $4s$ and $5s$. Lastly, we note that for the Cr atoms one plane away from the interface (Fig. 4), the largest change is in the population of the $3d_{z^2-r^2}$ state. The symmetry of this change is evident from the figure.

Surface and interface effects are confined to distances on the order of one layer spacing due to very effective metallic screening. This fact is clearly demonstrated for the interface in the charge density rearrangements depicted in Fig. 4. By two layers away there is virtually no change in the charge density resulting from breaking the interface. Similarly, contour plots of the total charge density for systems with slabs as large as nine layers (not shown) indicate that the charge density quickly approaches the bulk distribution within roughly one layer from the interface.

Figure 5 displays the calculated layer-projected densities of states (LDOS's) for the AlNi/Cr system at small and large interfacial separations on the left and right sides of the figure, respectively. Each panel corresponds to a layer of atoms and is labeled according to the atom type and its distance from the interface [i.e., Al(1) is the first Al atom from the interface]. The lowest panel in the figure [labeled (a)] corresponds to the central layer of the system and is a mirror symmetry plane. Thus, as previously stated, there is a total of five layers of NiAl sandwiched by two three-layer slabs of Cr.

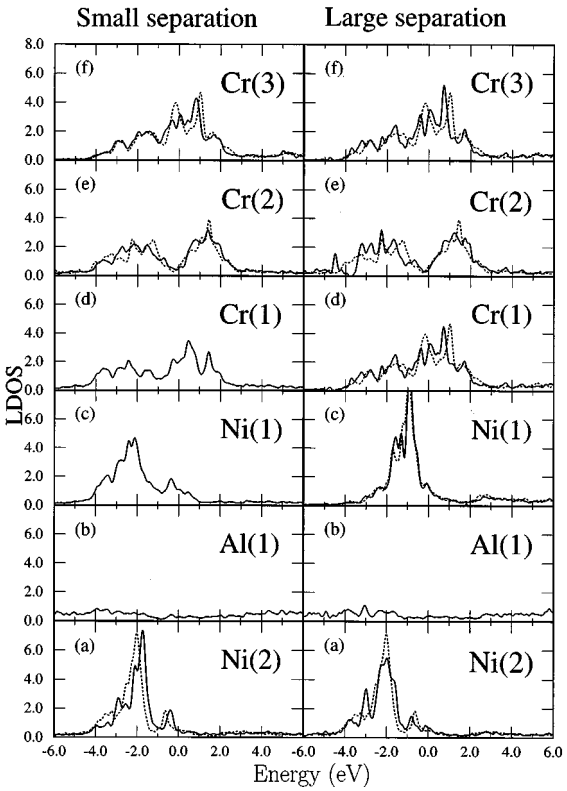

FIG. 5. Calculated layer-projected densities of states for the NiAl-Cr (AlNi/Cr) system at small interfacial separation ($a_0/2$) compared with those at large separation in units of states/(eV atom). The interface is between layers Ni(1) and Cr(1) [results displayed in panels (c) and (d) on the left for small separation ($a_0/2$) and on the right for the large separation]. The planes are labeled according to their atomic type and distance from the interface [i.e., Al(1) is the first Al layer from the interface]. The Fermi level defines the zero of energy and the dotted curves correspond to results calculated as described in the text. The close agreement between the solid and dashed curves justifies our use of thin slabs to model the interface.

Calculated electronic densities of states (DOS's) give further evidence in support of the claim that the interface between two thin slabs provides a good approximation to the NiAl-Cr interface. The solid curves are the calculated LDOS's for this system and the dashed curves correspond to the results obtained using thicker films. For a given layer, the dashed curves on the right and left are identical and correspond in panel(s) (f) to the LDOS from the surface layer of a nine-layer Cr system; in panel(s) (e) to the central layer of a nine-layer Cr system; and in panel(s) (a) to the central layer of a nine-layer NiAl system. The interfacial layers for the separated interface are free surfaces so we compare their LDOS's, in panel (d) and (c) at large separation, to the corresponding surface layers of the larger systems. In all cases the area under the LDOS curve is well reproduced by the thin-slab calculations. This implies that our results for total energies will be of good quality. In addition, we find good qualitative agreement for the density of states at the Fermi level and for the band filling.

The discrepancies between thin- and thick-slab results can be thought to arise from two sources: (1) a shift of the LDOS due to a change in the filling, and (2) additional structure for the smaller system due to quantum confinement. The central Ni layer provides a clear illustration of these two effects. In panel (a) the primary difference between the two curves from the Fermi level to -2.0 eV below E_f is simply a shift of roughly 0.25 eV. In the rigid band picture, this shift implies that isolated NiAl has slightly different band filling than does the system in which Cr is bonded to NiAl. This is a result of the fact that isolated NiAl has a different Fermi level than does Cr. In our calculations the Fermi levels of the two subsystems are equal. In order for this to occur there must be a slight separation-dependent charge transfer between the NiAl and Cr subsystems which manifests itself as a weakly separation-dependent band filling. Between -2.0 and -4.0 eV there is more structure for the smaller-slab calculation corresponding presumably to states due to confinement. In contrast to panel (a) on the left, in the equivalent panel on the right, the primary difference between the thick- and thin-slab calculations is due to the additional structure of the thin-slab system. The central peaks are now aligned in energy, demonstrating that, for the separated system, there is very little charge transfer. The primary effect of breaking the Ni-Cr interfacial bonds is the transference of weight from the central peak to the one at -3.0 eV.

The *d* electrons of Ni and Cr at the interface play a significant role in interfacial bonding and the bonding in NiAl is largely due to *sp-d* hybridization. Orbital-projected LDOS's (not shown) demonstrate that the contribution to the interfacial LDOS's [panels (c) and (d)] due to *s* and *p* states is of very small amplitude. Comparison between panels (e) and (d) for Cr and (a) and (c) for Ni shows that there is considerable broadening of the LDOS at the interface for Ni and a significant increase in the LDOS at E_f for Cr. These changes imply bonding. The spread in energy, of roughly 4.0 eV, indicates that the interfacial bonding states can be thought to be of an itinerant character. The LDOS for the Ni layer of the separated interface [panel (c) on the right] is narrower by roughly a factor of 2 in the absence of hybridization with the broad Cr band. The bonding in NiAl represents a situation in which the states are intermediate between localized and diffuse (itinerant). The bonding is due to a hybridization between the diffuse *sp* states of Al and the more localized states of Ni. An example of this coupling is the small bump in the Al LDOS of panel (b) on the right at -3.0 eV which corresponds to a similar feature at the same position in the LDOS of Ni in panel (a) on the right. The fact that a similar feature is found in both panels could, however, be merely an artifact of the Mulliken approximation.

C. Segregation effects on adhesion

Qualitatively different behavior may occur for slow and fast fracture of the interface due to the different adhesion curves for Ni-terminated (AlNi/Cr) and Al-terminated (NiAl/Cr) interfaces. Figure 1 shows that the lowest-energy interface is one in which the Cr is in contact with Ni. Since pure Al has a lower surface energy than Ni, however, the free NiAl surface tends to be Al terminated.[26] Thus for slow fracture (i.e., below the threshold for catastrophic failure) we expect the system to follow the AlNi/Cr adhesion curve (Fig. 1) until sufficient segregation has taken place to allow the system to follow the NiAl/Cr adhesion curve. Figure 1 shows that the AlNi/Cr and NiAl/Cr curves cross at roughly $d=2$ Å which is very close to the maximum of the stress vs separation curve of Fig. 2. This is the point at which the system will begin to follow the NiAl/Cr curve if the crack propagates very slowly.

We can estimate the segregation effect on the work of adhesion $W_{\rm ad}$ and peak interfacial stress $\sigma_{\rm max}$ by modifying the AlNi/Cr adhesion curve at large separation. The surface energy of pure Ni is 2664 mJ/m^2,[27,28] while the Al surface energy is 1170 mJ/m^2.[15,29] The difference of these two surface energies, 1494 mJ/m^2, gives a rough estimate of the change to the AlNi/Cr work of adhesion: $W_{\rm ad}^{\rm AlNi/Cr}=7388$ mJ/m^2 $\rightarrow W_{\rm ad}$(segregation)≈ 5894 mJ/m^2.

D. Comparison with previous studies

In experimental studies of fracture in NiAl-Cr composites it was found that cracks are resisted by, among many effects, crack bridging, crack deflection, and interfacial sources of mobile dislocations.[2] In the case of crack bridging, a crack in the NiAl matrix encounters a Cr fiber (or lamella) and its propagation is hindered in the Cr-rich phase, as indicated by wedge-shaped necks there. Often cracks have been observed to renucleate on the other side of a Cr fiber or lamella. If the interface is relatively weak, the crack can change its direction and travel along the interface. Mobile dislocations can be produced at the interface due to the difference in thermal expansion of the NiAl- and Cr-rich phases, as noted earlier. The most common toughening mechanism is crack bridging and the next most common is crack deflection, as observed experimentally.[2]

There has been some discussion in the literature[30,31] as to which quantity, the work of adhesion or the peak interfacial stress $\sigma_{\rm max}$, is more important for determining the fracture criterion. It has been argued that $\sigma_{\rm max}$ is critical to the strength of composites.[32] Recent theoretical studies suggest that the criterion for dislocation emission in a chemically embrittled solid is mostly determined by the nominal stress at fracture.[31] In a study of impurity effects on adhesion between Mo and $MoSi_2$, Hong *et al.* found that while $W_{\rm ad}$ was reduced for all impurities considered, some impurities such as C increased $\sigma_{\rm max}$ while others such as S caused it to decrease.[14] C is known to enhance cohesion in steels, while S is known to cause embrittlement.[33] To the extent that impurity embrittlement of steels and Mo composites is similar, these results suggest the relative importance of $\sigma_{\rm max}$. While the Griffith fracture strength depends only on $W_{\rm ad}$, [Eq. (1)], the theoretical strength $\sigma_{\rm max}$ depends not only on $W_{\rm ad}$ (or $E_0=W_{\rm ad}/2$) but also on the shape of the potential as described by the scaling length l [Eq. (5)]. Simply put, for a given value of the work of adhesion, the peak theoretical stress will be larger (smaller) if the energy vs separation decays more quickly (less quickly). This suggests that Eq. (5) is more general than the Griffith condition of Eq. (1).

We may estimate the contribution to the work of adhesion due to plastic work by comparing the calculated work of adhesion with the results of fracture toughness measurements.[2] The fracture toughness is the work required

to fracture the material, including the effects of plasticity. Although the relation between the work of adhesion and the plastic work is not known explicitly, there is a body of experimental and theoretical research which suggests that small changes in the work of adhesion can lead to large changes in the degree of plastic work. This is not surprising, since the maximum stress that can be applied to the material is ultimately limited by bond strengths at or near the crack tip. The difference between the measured fracture toughness and our calculated ideal work of adhesion is the work due to plasticity. For zone-refined $\langle 001 \rangle$ single-crystal NiAl, the fracture toughness is 11 MPa $m^{1/2}$.[2] To determine the corresponding fracture energy we appeal to the definition of the stress intensity factor:

$$K^2 = \frac{GE}{(1-\nu^2)}, \tag{6}$$

where G is the fracture energy (and is equal to W_{ad} in the absence of plastic deformation), E is Young's modulus, and ν is Poisson's ratio. For fracture along $\{001\}$ we use the measured values of $E_{001} = 95.9$ GPa and $\nu_{001} = 0.404$.[2] Using Eq. (6) and the measured value of the fracture toughness ($K = 11$ MPa $m^{1/2}$) we obtain $G = 1056$ J/m^2 for the fracture energy. Our calculated work of adhesion to separate the $\{001\}$ interface is 6.294 J/m^2. Thus we estimate the plastic work to be $W_p \approx 1050$ J/m^2, a value which is 167 times the ideal work of adhesion. For a brittle solid with limited crack-tip plasticity, such as a glass, the fracture toughness is typically on the order of 2 to 5 times the ideal work of adhesion.[34] This shows that NiAl exhibits considerable crack-tip plasticity despite the fact that it fails by brittle fracture. It should be noted that NiAl tends to fracture along $\{110\}$ planes rather than $\{001\}$ planes. This does not change the above argument qualitatively. It only implies that in principle we should be comparing a calculated work of adhesion for fracture along $\{110\}$ planes which will be smaller than for $\{001\}$ but will be of the same order of magnitude. Since the ideal work of adhesion is so much smaller than the one inferred from fracture toughness measurements, we would obtain the same conclusion: there is a significant amount of plasticity associated with the fracture.

NiAl-Cr eutectic composites are considerably tougher than NiAl due to the previously mentioned toughening mechanisms provided by the Cr phase. For comparison, the fracture toughness for the NiAl-Cr eutectic composite is 16.4 MPa $m^{1/2}$, which is 3.8 times greater than the fracture toughness of polycrystalline NiAl (4.3 MPa $m^{1/2}$).[2]

Our calculations of the electronic structure are consistent with previous investigations of the individual phases. Previous experimental[35,36] and theoretical[37] studies of the electronic charge density distribution indicate that NiAl forms strong covalent bonds between the Ni and Al atoms and these are superimposed on a metallic-bonding charge distribution. This type of bonding is similar to that between the Ni and Cr atoms at the NiAl-Cr interface as displayed in Fig. 4. We also find Ni d–Al p hybridization, a filled Ni d band, and low density of states at the Fermi level (Fig. 5) in accordance with previous first principles calculations.[38] The work of adhesion for NiAl has also been previously calculated from first principles[39] (5.5 J/m^2) and is in reasonable agreement with our result (6.3 J/m^2).

A very large body of experimental and theoretical work exists for Cr.[40] A number of first principles calculations have been performed to determine the electronic structure of Cr and are summarized in Ref. 40. To verify the accuracy of our method, we have repeated the calculations of Fu and Freeman[41] in which Cr was represented as a seven-layer slab with two free surfaces. We find good agreement with their calculations with the exception that our calculated value of the work function is somewhat smaller than that of Ref. 41. These authors report a value of 4.4 eV for the paramagnetic state of Cr while we obtain 3.9 eV. The difference could be due to the fact that we are using a different exchange-correlation potential (we used Ceperley-Alder[18] while Fu and Freeman used Hedin-Lundqvist[42]). Similar discrepancies exist in the measured values of the Cr work function. Wilson and Mills[43] obtained 4.46 eV while Meier *et al.*[44] obtained 4.1 eV. Skriver and Rosengaard have calculated the work function for a larger number of elements[45,46] from first principles. Their result for Cr is larger than 5 eV (5.45 eV for the $\{110\}$ surface; no result is presented for the $\{001\}$ surface).

Several authors have calculated surface energies for Cr from first principles.[45,47] For the $\{001\}$ surface, the calculated value including magnetic effects (Fig. 1 of Ref. 47) is close to the experimental value of 2.3 J/m^2 which was derived from measurements of surface tensions of liquid metals.. Their calculated surface energy for $\{110\}$ Cr is 3.63 J/m^2. Our calculated value of the surface energy (i.e., $W_{ad}/2$)is 4.8 J/m^2. It is possible that our overestimate of this quantity is due to the neglect of magnetic effects which Aldén *et al.* have shown to be important.[47] These authors have shown that upon including magnetism substantial reductions in the surface energy can occur. We are currently carrying out local spin-density functional (LSD) calculations for the AlNi/Cr system, which will include magnetic effects.

IV. CONCLUSIONS

We have presented first principles calculations of the work of adhesion and peak interfacial stress for NiAl, Cr, and NiAl-Cr interfaces, along with charge density rearrangements and densities of states. We find that Cr has the largest work of adhesion and peak interfacial stress, NiAl has the lowest, and the interface has an intermediate value. Our calculations indicate that NiAl at the NiAl-Cr interface is Ni-terminated. This leads to the suggestion that there may be a qualitative difference between slow and fast fracture due to segregation effects since the free NiAl surface tends to be Al-terminated. Segregation effects which lower the NiAl surface energy have been estimated to reduce the work of adhesion of the interface by roughly 20%. Calculations of electronic charge density rearrangements indicate that the interfacial bonding is metallic with a significant covalent character. This situation was also found in previous experimental and theoretical studies for the bonding between the Ni and Al atoms in NiAl. The bonding at the interface was found to be due to the $3d$ as well as $4s$, $4p$, and $5s$ electrons of the Ni and Cr atoms and that in NiAl is due to Ni d-Al p hybridization. Comparisons between the calculated

ideal work of adhesion and fracture toughness measurements show that NiAl has significant crack-tip plasticity despite the fact that it fails by brittle fracture. Since the ideal work of adhesion is often difficult to measure, first-principles calculations lead to a deeper insight into fracture problems by establishing trends through comparison with experimental results.

ACKNOWLEDGMENTS

We would like to thank Ron Gibala for many helpful discussions. This work was supported by the U.S. Air Force Office of Scientific Research. Computational resources were provided by the San Diego, the Lawrence Livermore, and NASA-Lewis Supercomputing Facilities.

*Present address: Deptartment of Physics and Astronomy, Louisiana State University, Baton Rouge, LA 70803.

[1] X. F. Chen, D. R. Johnson, R. D. Noebe, and B. F. Oliver, J. Mater. Res. **10**, 1159 (1995).
[2] D. R. Johnson, X. F. Chen, B. F. Oliver, R. D. Noebe, and J. D. Whittenberger, Intermetallics **3**, 99 (1995).
[3] R. Darolia, J. Met. **43**, 44 (1991).
[4] D. B. Miracle, Acta Metall. **41**, 649 (1993).
[5] R. D. Noebe, R. R. Bowman, and M. V. Nathal, Int. Mater. Rev. **38**, 193 (1993).
[6] J. L. Walter and H. E. Cline, Metall. Trans. **1**, 1221 (1970).
[7] H. E. Cline and J. L. Walter, Metall. Trans. **1**, 2907 (1970).
[8] J. L. Walter and H. E. Cline, Metall. Trans. **4**, 33 (1973).
[9] J. L. Walter, H. E. Cline, and E. F. Koch, Trans. AIME **245**, 2073 (1969).
[10] H. E. Cline, J. L. Walter, E. F. Koch, and L. M. Osika, Acta Metall. **19**, 405 (1971).
[11] S. M. Merchant and M. R. Notis, Mater. Sci. Eng. **66**, 47 (1984).
[12] A. A. Griffith, Philos. Trans. R. Soc. London Ser. A **221**, 163 (1920).
[13] T. Hong, J. R. Smith, D. J. Srolovitz, J. G. Gay, and R. Richter, Phys. Rev. B **45**, 8775 (1992).
[14] T. Hong, J. R. Smith, and D. J. Srolovitz, Phys. Rev. B **47**, 13 615 (1993).
[15] T. Hong, J. R. Smith, and D. J. Srolovitz, J. Adhesion Sci. Technol. **8**, 837 (1994).
[16] P. Hohenberg and W. Kohn, Phys. Rev. **136**, 864 (1964); W. Kohn and L. J. Sham, *ibid*. **140**, A1133 (1965).
[17] U. von Barth and C. D. Gelatt, Phys. Rev. B **21**, 2222 (1980).
[18] D. M. Ceperley and B. J. Alder, Phys. Rev. Lett. **45**, 566 (1980).
[19] J. R. Smith, J. G. Gay, and F. J. Arlinghaus, Phys. Rev. B **21**, 2201 (1980).
[20] A. Banerjea and J. R. Smith, Phys. Rev. B **37**, 6632 (1988); see also P. Vinet, J. H. Rose, J. Ferrante, and J. R. Smith, J. Phys. Condens. Matter **1**, 1941 (1989).
[21] J. P. Perdew in *Electronic Structure of Solids '91*, edited by P. Ziesche and H. Eschrig (Akademie Verlag, Berlin, 1991), pp. 11–20.
[22] J. P. Perdew, J. A. Chevary, S. H. Vosko, K. A. Jackson, M. R. Pederson, D. J. Singh, and C. Fiolhais, Phys. Rev. B **46**, 6671 (1992).
[23] J. P. Perdew and K. Burke, Int. J. Quantum Chem. **57**, 309 (1996), and references within.
[24] R. S. Mulliken, J. Chem. Phys. **23**, 1833 (1955).
[25] For an enlightening discussion of bonding in transition metals, see C. D. Gellatt, Jr., H. Ehrenreich, and R. E. Watson, Phys. Rev. B **15**, 1613 (1977).
[26] Actually the surface is composed of 65% Al atoms and 35% Ni atoms (see Sec. 3.3.3 of Ref. 4). See, however, Ref. 5, p. 197, where it is stated that the NiAl{001} surface, which we treat here, has a maximum of 22% Ni present in the surface atomic layer.
[27] H. Wawra, Z. Metallkd. **66**, 375 (1974).
[28] R. Richter, J. R. Smith, and J. G. Gay, in *The Structure of Surfaces*, edited by M. A. Van Hove and S. Y. Tong (Springer-Verlag, New York, 1983), p. 35.
[29] H. Wawra, Z. Metallkd. **66**, 395, (1975); **66**, 492 (1975).
[30] E. Orowan, Rep. Prog. Phys. **12**, 194 (1949).
[31] R. Thomson (private communication).
[32] W. J. Baxter, Metall. Trans. **23A**, 3045 (1992).
[33] J. R. Rice and J.-S. Wang, Mater. Sci. Eng. A **107**, 23 (1989).
[34] T. H. Courtney, *Mechanical Behavior of Materials* (McGraw-Hill, New York, 1990), p. 423.
[35] A. G. Fox, in *Electron Microscopy and Analysis*, edited by G. J. Tatlock, IOP Conf. Proc. No. 78 (Adam Hilger, Bristol, 1985), p. 379.
[36] A. G. Fox and M. A. Tabbernor, Acta Metall. **39**, 669 (1991).
[37] C. L. Fu and M. H. Yoo, in *High Temperature Ordered Intermetallic Alloys IV*, edited by L. Johnson, D. P. Pope and J. O. Steigler, MRS Symposia Proceedings No. 213 (Materials Research Society, Pittsburgh, 1991), p. 667.
[38] S.-C. Lui, J. W. Davenport, E. W. Plummer, D. M. Zehner, and B. W. Fernando, Phys. Rev. B **42**, 1582 (1990).
[39] M. H. Yoo and C. L. Fu, Scr. Metall. Mater. **25**, 2345 (1991).
[40] E. Fawcett, Rev. Mod. Phys. **60**, 209 (1988).
[41] C. L. Fu and A. J. Freeman, Phys. Rev. B **33**, 1755 (1986).
[42] L. Hedin and B. I. Lundqvist, J. Phys. C **4**, 2064 (1971).
[43] R. J. Wilson and A. J. Mills, Jr., Surf. Sci. **128**, 70 (1983).
[44] F. Meier, D. Pescia, and T. Schriber, Phys. Rev. Lett. **48**, 645 (1982).
[45] H. L. Skriver and N. M. Rosengaard, Phys. Rev. B **45**, 9410 (1992).
[46] H. L. Skriver and N. M. Rosengaard, Phys. Rev. B **46**, 7157 (1992).
[47] M. Aldén, H. L. Skriver, S. Mirbt, and B. Johansson, Phys. Rev. Lett. **69**, 2296 (1992).